THE JOURNAL OF PHYSICAL CHEMISTRY B

ARTICLE

pubs.acs.org/JPCB

Fluorine Environment in Bioactive Glasses: *ab Initio* Molecular Dynamics Simulations

Jamieson K. Christie,[†] Alfonso Pedone,[§,‡] Maria Cristina Menziani,[∥] and Antonio Tilocca[*,†]

[†]Department of Chemistry and Thomas Young Centre, University College London, London WC1H 0AJ, U.K.

[‡]Scuola Normale Superiore di Pisa, 41100 Pisa, Italy

[∥]Department of Chemistry, Università di Modena e Reggio Emilia, 41100 Modena, Italy

ABSTRACT: Fluorinated bioactive glasses (FBGs) combine the antibacterial properties of fluorine with the biological activity of phosphosilicate glasses. Because their biomedical application depends on the release of fluorine, the detailed characterization of the fluorine environment in FBGs is the key to understand their properties. Car−Parrinello molecular dynamics (CPMD) simulations have been performed on a 45S5 Bioglass composition in which 10 mol % of the CaO has been replaced with CaF_2, and have allowed us to resolve some longstanding issues about the atomic structure of fluorinated bioglasses, with particular regard to the structural role of fluorine. F is coordinated almost entirely to the modifier ions Na and Ca, with a very small amount of residual Si−F bonds, whose fraction only becomes significant in the melt precursor. High temperature leads to Si−F bonds in both tetra- (SiO_3F) and, less frequently, penta-coordinated (SiO_4F and SiO_3F_2) complexes, showing that formation of these bonds through the expansion of the SiO_4 coordination shell is generally less favored. There is no evidence for preferential bonding of F to either modifier ion: almost all F atoms are coordinated to both calcium and sodium in a "mixed state", rather than exclusively to either, as had been conjectured. We discuss the consequences of these findings on the properties of fluorine-containing bioglasses.

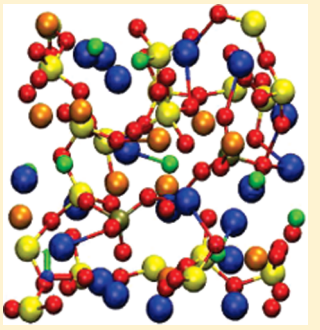

INTRODUCTION

Fluoride is known to protect against dental caries (tooth decay) by inhibiting tooth enamel demineralization, enhancing remineralization and inhibiting bacterial enzymes.[1] When fluoride is present during enamel remineralization, it forms fluorapatite, which is much less susceptible to acid attack than hydroxyapatite (HA), the main component of tooth enamel.[1] Bioactive glasses (BGs) are known to form a surface layer of HA when implanted in the body;[2] further transformation of this layer eventually leads to a chemical bond between the glass and the bone: bone-bonding BGs are clinically employed in dental and other low load-bearing implants.[3] There is thus high interest in combining the bone-bonding properties of BG and the anticariogenic protection of fluorine in fluorinated bioglasses (FBGs). Because the biomedical applications of these materials critically depend on the release of ionic species (fluoride in particular) in the surrounding physiological environment, it is vital to obtain a very accurate picture of the structural organization around fluorine. Several previous studies have focused on the effect of fluorine inclusion into bioactive and other silicate glasses, with somewhat contradictory results.[4−14] In particular, two questions are still not wholly resolved: what is the prevalence of fluorine bonding to silicon, and in the presence of more than one modifier species (as in bioglass, which has two: sodium and calcium), how does flourine prefer to bond to them?

Atomic environments in silicate glasses can be effectively probed through solid-state nuclear magnetic resonance (NMR):[15] multinuclear experiments,[16] also combined with cross-polarization and *J*-mediated techniques,[17,18] are frequently needed to obtain valuable information on the short-range glass structure, overcoming resolution problems due to the range of different local environments found in a disordered system. ^{19}F magic-angle spinning (MAS) NMR has proven adequate to characterize fluorine environments in multicomponent compounds.[5,19]

Wood and Hill[4] observed a decrease in glass transition temperature T_g with increasing F content in F-containing calcium aluminosilicate glasses, which they interpreted as some of the F disrupting the network by replacing Si−O−Si bonds with two Si−F bonds. Si−F bonds were also observed in ^{19}F MAS NMR studies of F-containing sodium silicate glass,[5] although none were seen in ^{19}F MAS NMR studies of potassium, calcium or lanthanum silicate glasses.[5,6] ^{19}F MAS NMR studies of aluminosilicate glasses containing calcium and other ions,[7,8] showed the presence of Al−F bonds in high-F content glasses, and Si−F only in very high-F content, indicating that if both Al and Si are present, Al−F bonds are preferred. ^{19}F MAS NMR and $^{19}F-^{27}Al$ cross-polarization NMR showed the presence of Al−F

Received: November 11, 2010
Revised: January 14, 2011
Published: February 15, 2011

bonds involving 4-, 5- and 6-coordinated Al in aluminate glasses.[9] On the other hand, classical (based on empirical force fields) simulations of alkaline earth silicate glasses[10] suggested that Si−F bonds exist only in more acidic environments, e.g., when Ba is the modifier, and they were absent when the modifier was Ca, Sr, or Pb.[11] Moreover, a recent ^{19}F and ^{29}Si MAS NMR study[12] specifically of F-containing BG showed that the proportions of Si−F bonds and nonbridging fluorine (NBF) atoms are small, if not zero. These controversial results could indeed reflect the presence of only a low proportion of Si−F bonds, which hinders the experimental characterization of their environment.

Another issue involves the way in which fluorine can be incorporated in the silicon coordination shell in the glass: for instance, it is possible that fluorine replaces oxygen, maintaining a four-coordinated Si environment, but it is also possible that the addition of an Si−F bond expands Si's first coordination shell to five neighbors. A simulation of barium-containing silicate glass[10] did highlight such an expansion, with elongated Si−F bonds in a trigonal bipyramidal structure around the five-coordinated silicon atom, and a similar coordination is also found in different siliceous zeolites from a combination of ^{19}F MAS NMR and X-ray diffraction,[21,23] classical[20,24] and first-principles[22] simulations, with Si−F bond lengths ranging from 1.75 to 2.10 Å. It is clear that a range of Si−F bonding environments is potentially possible in fluorinated BG.

Turning to the F−M coordination, where M is a modifier atom, FCa_n clusters were identified from diffraction[4] and MAS NMR[7,8] on F-containing calcium aluminosilicate and calcium silicate[6] glasses. For glasses containing more than one modifier, Stebbins and Zeng's NMR experiments[5] observed a wide variety of F environments, and although "much or most of the F^- sites have mixed cation environments", they observed a preference for fluorine to bond to modifiers with higher field strengths, where the field strength of an ion is defined as its valence divided by the square of the bond length to its oxygen neighbor when six-coordinated (lower field strengths thus characterize ions with stronger network-modifying properties). This would imply a preference for F−Ca (the Ca field strength is 0.33) over F−Na (the Na field strength is 0.19) interactions in F-containing bioglass. NMR studies of aluminosilicate glasses containing both calcium and sodium exhibited peaks attributed to FCa_n and Al−FCa_n clusters, and a weaker peak attributed[8] to the presence of Al−FNa_n clusters; however, they also emphasized that the presence of mixed bonding states is likely. A recent NMR study[12] suggested that fluorine is mainly present in mixed states, coordinated to both sodium and calcium.

A better understanding of these features, based on atomistic simulations, could support the interpretation of the different surface reactivity shown by fluorinated BG, compared to F-free bioglass.[13] In particular, earlier studies on soda lime phosphosilicate bioactive glasses showed that the addition of fluorides (CaF_2) decreases the chemical reactivity, because F seems to inhibit the formation of a thick surface gel layer with a high silica concentration,[25] a key feature in the well-established mechanism for the formation of HA.[26] Subsequent *in vitro* and *in vivo* studies on short-term bone implants of fluorinated glasses confirmed that the silica gel layer deposited on FBGs is not as homogeneous as that formed on a similar F-free bioglass,[27] and in some cases is small or absent.[14,28] However, the lack of a continuous Si-rich layer does not seem to affect the ability of the FBG glass surface to eventually become covered with a deposited layer of hydroxy- and fluoroapatite crystal phases.[14]

A recent classical molecular dynamics (MD) study by some of us[29] showed that F in bioactive glasses is coordinated almost exclusively to the network modifiers Na and Ca, with no clear preference for either ion. No significant concentration of Si−F bonds was observed, with only very few (<2%) of such bonds observed in the glasses with the highest fluorine content. The absence of Si−F bonds, and the corresponding preferential association of fluoride to sodium and calcium, could represent the key feature of these systems. If verified, it would lead on a larger scale to fluoride being found almost exclusively in regions populated with calcium and sodium cations, and well separated from the silicate network. This would bear important consequences on the dissolution of F anions from the glass and its surface reactivity, which would also be affected by the relative weight of Na−F and Ca−F interactions in the fluoride-rich regions.

Given the huge importance of these features, it is vital to corroborate the classical MD results with additional independent data on the structure of FBGs. Classical MD simulations allows us to study relatively large models, and directly obtain information on the medium-range structure of glasses, such as the network connectivity.[30] However, classical MD is always limited by the accuracy of the force field chosen. *Ab initio* (AI) simulation is much more computationally intensive, and hence restricted to much smaller models, however, its parameter-free nature provides a suitable way to obtain completely unbiased structural models of glasses[31,32] The combination of classical and *ab initio* (AI) simulation methods[33,34] represents a very powerful tool to investigate complex systems such as BGs on different scales. The good degree of complementarity between these techniques can be exploited to develop and interpret large-scale models built through the detailed insight obtained from smaller-scale AI models,[35] or to assess and validate particular features emerged from the classical models themselves.[31,36] For the present problem, the relatively small size of the AIMD models is adequate to investigate the local structure, such as the coordination environment of fluoride, with high accuracy.

In this work, we present AIMD simulations of a representative FBG composition, with the purpose to assess the proposed low tendency of fluoride to form Si−F bonds, with a corresponding preference for associating with Na and Ca modifier ions, and provide new insight on the actual F environment in modifier ion-rich regions.

■ COMPUTATIONAL PROCEDURE

CPMD simulations were carried out using the CP code of the Quantum-ESPRESSO package,[37] using the generalized gradient approximation (GGA) to density-functional theory (DFT),[38] ultrasoft pseudopotentials,[39] and a plane-wave basis set with cutoffs of 30 and 240 Ry for the smooth part of the wave functions and the augmented charge, respectively. *k*-point sampling included the Γ point only. The time step and fictitious electronic mass were 0.17 fs and 400 atomic units, respectively. Periodic boundary conditions were used throughout. This computational framework has previously proven suitable to model the short-range structure of fluorine-free modified silicate glasses[32,40,41] and of bioactive glasses.[31,36,42,43]

Three independent configurations were generated, each corresponding to 45S5 Bioglass in which 10 mol % CaO of the bioglass composition has been replaced by CaF_2 (composition "$HCaCaF_2$ 10%" in ref 29) Each initial configuration was

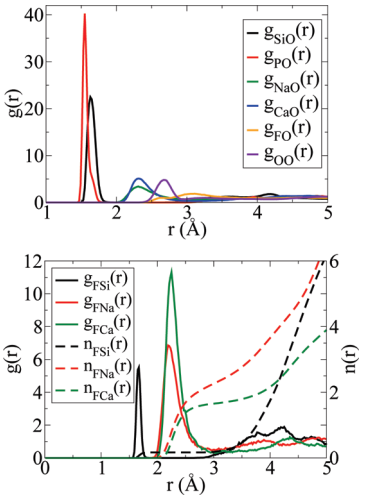

Figure 1. Partial pair-distribution functions $g_{XO}(r)$ (top) and $g_{FX}(r)$ (bottom, solid line), and running coordination numbers $n_{FX}(r)$ (bottom, dashed line), averaged over the three models.

Table 1. Coordination Numbers of Various Cation−Anion Pairs, Averaged Over the Three Models[a]

X	X−O	X−BO	X−NBO	X−F	X total
Si	3.94	2.33	1.61	0.07	4.01
P	4.00	0.67	3.33	0.00	4.00
Na	5.10	1.52	3.59	0.97	6.07
Ca	5.28	0.83	4.45	1.23	6.50
	F−Si	F−P	F−Na	F−Ca	F total
	0.17	0.00	2.41	1.69	4.27

[a] BO and NBO denote bridging and nonbridging oxygen atoms respectively. The cutoff for coordination to Si and P atoms is 2.0 Å and to Na and Ca atoms is 3.2 Å.

obtained by randomly placing 120 atoms (comprising 19 SiO_2, 10 Na_2O, 1 P_2O_5, 4 CaF_2, and 7 CaO formula units) into a cubic box of side 11.74 Å, corresponding to the experimental density of 2.695 g cm^{-3}.[29] To avoid unphysical starting configurations, atoms were not placed closer than 80−90% of their estimated interatomic distances. Each random configuration was used to start a CPMD run in the *NVT* (constant number of particles, volume, and temperature) ensemble at 3000 K, for such a time (typically ∼20 ps) as it took to establish that the model was well equilibrated, which was checked by directly examining the mean-square atomic displacements. Then each model was run for 10 ps in the *NVT* ensemble at each of 2500, 2000, 1000, and 300 K, corresponding to an effective cooling rate of ∼67 K/ps. The cooling rate used to produce melt-derived computer models of glasses is of course much faster than that used in experiment: however, simulated cooling rates of this order of magnitude are routinely used in both computationally cheaper classical MD simulations,[30,44−46] and fully *ab initio* simulation of other glasses,[32,47−49] including the F-free counterpart to this bioglass composition, 45S5 bioglass.[31] After the cooling phase, a final trajectory in the NVE (constant number of particles, volume and energy) ensemble was run for 10 ps, with average temperatures between 280 and 320 K for the three independent samples. Unless otherwise stated, all data presented in this paper are averaged over evenly spaced configurations taken from the NVE trajectory, and further averaged over the three models.

Table 2. Coordination Numbers of Silicon, Sodium, and Calcium to Fluorine at Various Temperatures and Cutoffs, Averaged over the Three Models

species	cutoff (Å)	300 K	1000 K	2000 K	2500 K	3000 K
Si−F	2.0	0.07	0.06	0.07	0.11	0.11
Si−F	2.3	0.07	0.06	0.08	0.12	0.14
Na−F	3.2	0.97	0.97	0.89	0.87	0.90
Na−F	3.5	1.10	1.10	1.03	1.02	1.06
Ca−F	3.2	1.23	1.24	1.23	1.16	0.96
Ca−F	3.5	1.29	1.32	1.35	1.31	1.08

Table 3. Percentage of Silicon Atoms with a Given Coordination Number to Both Oxygen and Fluorine Atoms, Averaged over the Three Models, As a Function of Temperature, with a Cutoff of 2.3 Å

Si−O,F CN	300 K	1000 K	2000 K	2500 K	3000 K
2	0	0	0	0	0.3
3	0	0	0.5	1.9	5.0
4	99.3	97.9	96.1	90.3	84.9
5	0.7	2.1	3.3	7.6	9.3
6	0	0	0.1	0.2	0.4

RESULTS

Local Structure. F-free bioglasses (BGs) have been the subject of many simulations, and their structure is now relatively well understood.[33] Several structural properties of the present FBG models reflect general features of BGs. Figure 1 (top) shows the radial distribution functions, $g(r)$, for all species with oxygen in our models. The first peaks are the P−O (1.55 Å) and the Si−O (1.63 Å) bond lengths. These peaks are very sharp, indicating considerable uniformity in these bonds. Table 1 shows that the Si−O and P−O coordination numbers are both very close to 4. At larger distances, the Na−O and Ca−O distributions are peaked at 2.31 Å. These peaks are wider, indicating more disorder in the Na and Ca environments. Because of their roles as network modifiers, Na and Ca are mostly coordinated by nonbridging oxygen (NBO) atoms (Table 1): the Na−O coordination number is 5.1, of which 3.6 are NBO, and the Ca−O coordination number is 5.3, of which 4.5 are NBO. The O−O first peak appears at larger distances (2.67 Å). This peak mainly corresponds to O−P−O (2.55 Å) and O−Si−O (2.69 Å) distances, although there are also non-negligible contributions from O−Na−O (2.65 Å) and O−Ca−O (2.63 Å).

These values fall well within the range of corresponding distances measured by X-ray and neutron diffraction in the F-free composition,[50] showing that the inclusion of fluorine does not significantly affect the oxygen coordination polyhedra on the short-range scale. On the other hand, fluorine affects the medium-range connectivity between these polyhedra to a much greater extent; whereas the small number of P atoms in the present samples prevents a quantitative analysis of the P environment, the presence of Si−O−P bridges involving about two-thirds of the P atoms is in qualitative agreement with previous

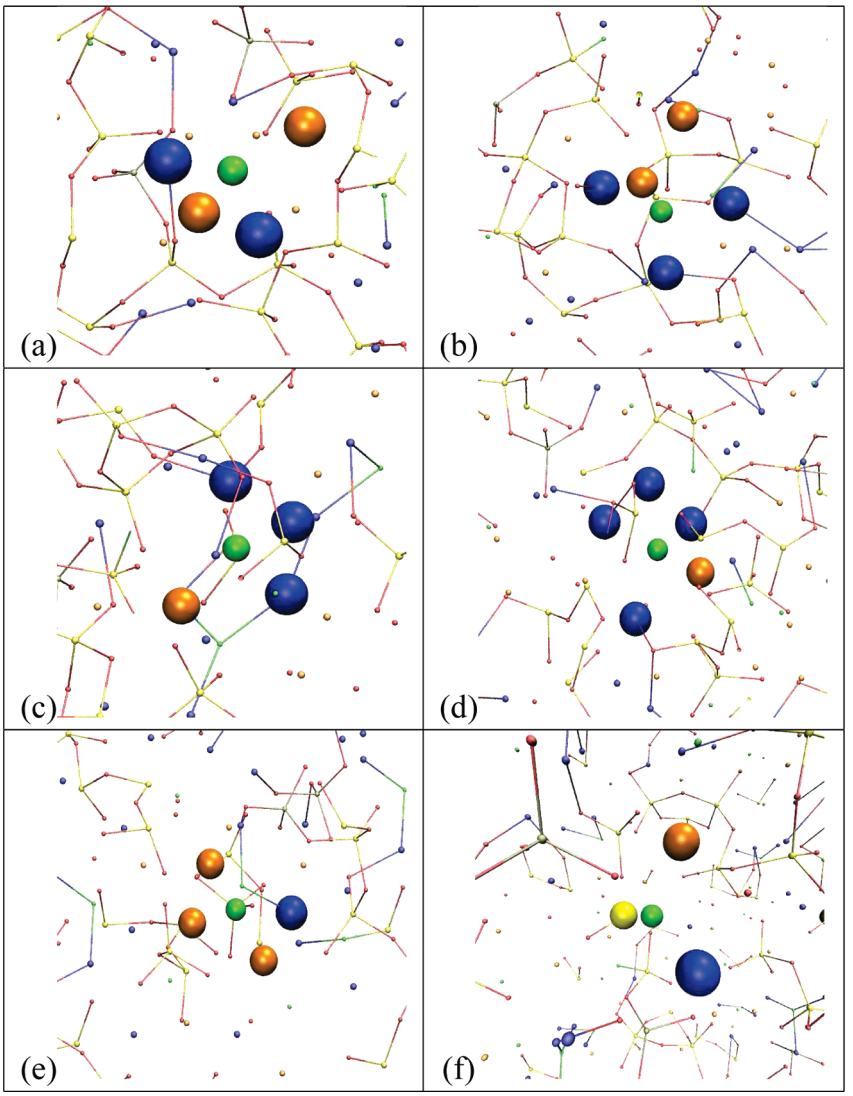

Figure 2. The most common fluorine environments (with abundances above 4%): (a) FNa_2Ca_2 (29% abundance), (b) FNa_3Ca_2 (18%), (c) FNa_3Ca (12%), (d) FNa_4Ca (6.9%), (e) $FNaCa_3$ (6.0%), and (f) FSiNaCa (4.1%). Fluorine, sodium, calcium, and silicon atoms are represented as green, blue, orange, and yellow spheres, respectively. Atoms other than the central fluorine and its first neighbor shell have been reduced in size for clarity.

simulations, which revealed a net increase in the Si−P connectivity in the present composition, compared to the F-free bioglass .[29]

Fluorine Association with Silicon. Radial distribution functions involving fluorine and the corresponding running coordination numbers $n(r)$ are given in Figure 1 (bottom). The first peak (1.67 Å) is the F−Si distance. There are very few F−Si bonds (about 2% of the bonds formed by Si), hence the low coordination number: $n(F-Si) = 0.17$ in Table 1, denoting that only 0.17 Si atoms are found within the first coordination shell of fluorine, on average. There are no F−P bonds, and $g_{FP}(r)$ (not shown) is zero at distances lower than 3.2 Å.

This *ab initio* evidence thus explicitly supports previous classical MD studies[29] which found Si−F bonds only at higher F concentrations than simulated here, as well as the most recent experimental results,[12] which showed that the fraction of Si−F bonds is small, if not zero. At the same time, these results are in contrast with previous suggestions, based on glass transition temperature and NMR data, which seemed to show that F disrupts the glass network by replacing Si−O−Si bridges with terminal Si−F bonds.[4,5] It is worth mentionting that no Si−F signal was seen in more recent NMR measurements.[12]

Furthermore, for the small amount of Si−F bonds identified, the present results support a model in which F replaces one of the O atoms in the Si coordination shell, rather than expanding the coordination shell itself with an additional Si−F bond, as previously proposed[10] and observed in some zeolites.[21,51] In particular, we find that 99.3% of the Si atoms are four-coordinated (Table 3), and the nearest-neighbor Si−F distance is strongly peaked at 1.67 Å (Figure 1 (bottom)), a distance comparable to the Si−O bond length of 1.63 Å (1 (top)). This implies that the very few instances of Si−F bonds formed in fluorinated bioglasses involve oxygen replacement by fluorine within the tetrahedral shell of Si. In other words, the low tendency of silicon to achieve 5- or 6-fold coordination in FBG glasses (at variance with other silicate phases[52]) hinders an alternative route toward Si−F bonds and thus significantly limits their occurrence.

Fluorine Association with Na and Ca. The two bands centered at 2.19 and 2.25 Å in the bottom panel of Figure 1

dx.doi.org/10.1021/jp110788h |*J. Phys. Chem. B* 2011, 115, 2038–2045

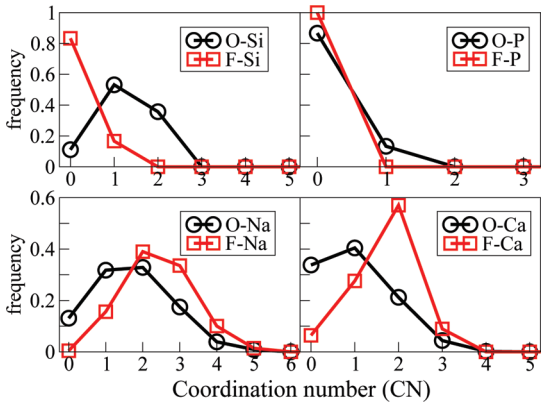

Figure 3. Distributions of oxygen-cation (black circles) and fluorine-cation (red squares) coordination numbers.

identify the characteristic Na−F and Ca−F distances for FBGs, and their large area denotes significant coordination of both modifier ions to fluorine. From Table 1, we see that, on average, each Na atom is coordinated to ∼1 F atom, and each Ca atom is coordinated to ∼1.2 F atoms. The F−F and O−F radial distribution functions (not shown) are characterized by a first peak at about 3 Å; the O−F distribution has a shoulder at ∼2.5 Å, corresponding to the small proportion of O−Si−F environments, whereas most of the F−F peak corresponds to F−(Na, Ca)−F distances.

The average F−Na and F−Ca coordination numbers are 2.4 and 1.7, respectively (Table 1). Due to the relatively small system size, it is important to estimate the error on these coordination numbers: we do this by observing that the standard deviation of the F−Na and F−Ca coordination numbers calculated from their values in each of the three independent models is typically about 10% of the coordination number itself. In each of our models, there are 10 Na and seven Ca atoms. The ratio of coordination numbers (CN): CN(F−Na)/CN(F−Ca) is 1.4 ± 0.2, close to the ratio of the number of atoms in the model, $N(\mathrm{Na})/N(\mathrm{Ca}) = 1.43$. Hence the F atoms are coordinated to the modifiers in similar (statistical) proportions to their abundance in the models, and we see no evidence of preferential association of F to either Na or Ca. This agrees with recent experimental data,[12] in contrast with previous data suggesting a preference for F to associate to higher-field-strength cations,[5] although we note that the latter experiment did not involve a bioglass composition.

The most common F coordination shells—those with abundances above 4%—are shown in Figure 2 and do reflect mixed bonding to both Na and Ca. On average, our samples contain only a very small fraction (0.2%) of F atoms coordinated exclusively to Ca, and none coordinated exclusively to Na. This denotes that the separation of $F-Na_n$ or $F-Ca_n$ aggregates is unfavorable in this composition, and that essentially all F atoms prefer mixed states. This also applies to the very small number of F atoms bonded to Si: the ratio of the Si−F−Na/Si−F−Ca bonds is roughly consistent with the expected ratio if there were no preferential association.

The recent ^{19}F NMR data on FBG mentioned above[12] show a series of overlapping broad peaks, with shape depending on composition. For compositions close to that studied here, three peaks are seen, one of which is assigned to F atoms bonded to two Na and two Ca (FNa_2Ca_2), which is the most common F environment found in our simulations (Figure 2a). One of the

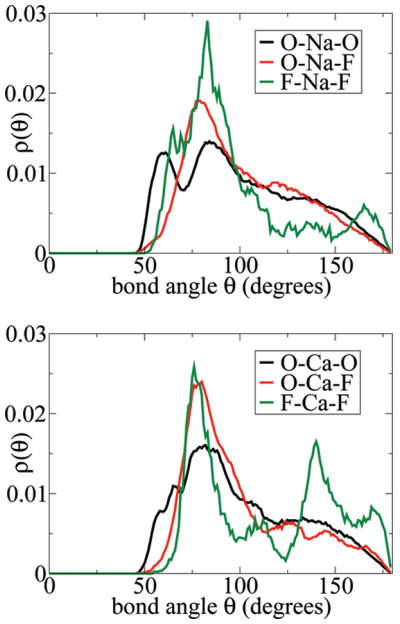

Figure 4. Bond-angle distributions centered on sodium (top) and calcium (bottom) modifier ions.

other peaks is attributed to overlapping signals from FCa_4 and $FNaCa_3$. While we find essentially no FCa_4 in our models, $FNaCa_3$ is also one of the most common environments in our models; see Figure 2e. The third NMR peak is assigned to F bonded to sodium.[12] While we find no F bonded *exclusively* to Na, all the most common fluorine environments identified in Figure 2 contain one or more sodium atoms coordinated to F.

The preference of fluorine to associate with Na and Ca certainly reflects more favorable F−Na(Ca) interactions, compared to F−Si(P). Whereas in principle one could perform simple quantum-mechanical calculations of representative gas-phase reactions to assess the thermodynamics of the fluorine association and quantitatively corroborate this suggestion, these calculations would have to take into account each component of the large array of chemical environments encountered by a fluorine atom in the glass, some of which were highlighted above. The extensive thermal averaging of our room-temperature trajectories provides a rigorous and *direct* way to sample each accessible molecular environment, with an appropriate statistical weight which intrinsically reflects the underlying thermodynamics within the high accuracy of the ab initio framework adopted. Even though the structural properties analyzed here provide an exhaustive picture of the fluorine environment in bioglasses, further work could involve structural optimizations of an adequate number of small clusters extracted from the MD trajectory, in order to assess the energetic balance of the individual F−Na, F−Ca, F−Si and F−P interactions.

Oxygen vs Fluorine Coordination Environments. Figure 3 Shows the distributions of the oxygen and fluorine coordination numbers. The very low number of F−Si bonds, as discussed above, leads to a very different distribution compared to the O−Si one, where most oxygen atoms are bonded to one or two silicon atoms. Flourine's preference for modifier atoms is also clear: the F−Na and F−Ca coordination-number distributions are noticeably shifted to higher coordination numbers than the O−Na and O−Ca distributions, respectively. Whereas significant fractions (13% and 34%, respectively) of O atoms are *not*

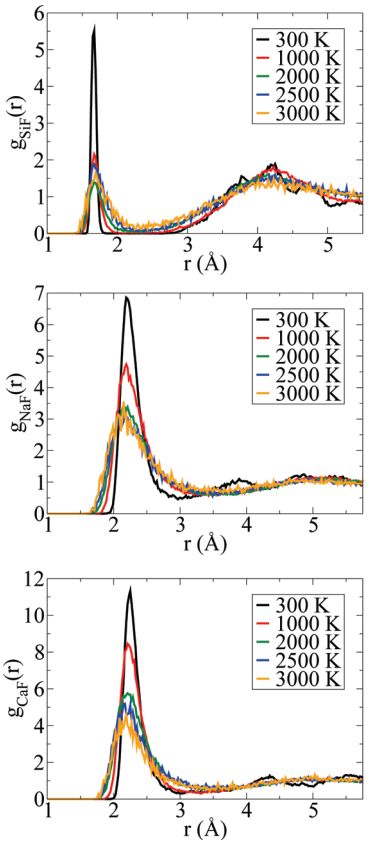

Figure 5. Radial distribution functions $g_{SiF}(r)$ (top), $g_{NaF}(r)$ (middle), and $g_{CaF}(r)$ (bottom) at different temperatures.

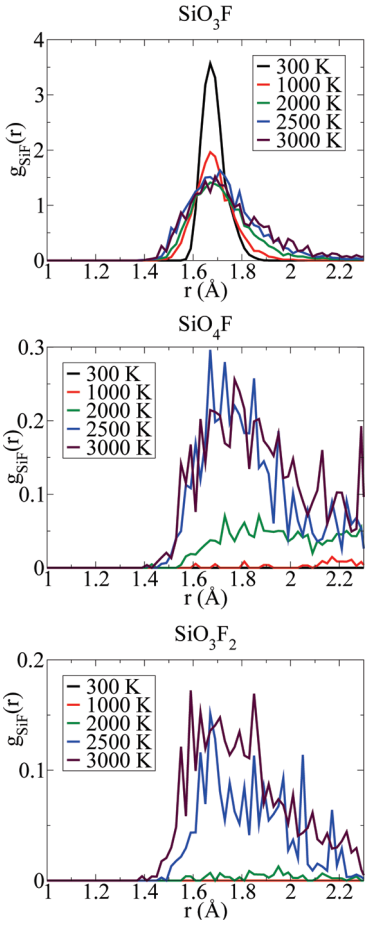

Figure 6. Radial distribution functions $g_{SiF}(r)$ for silicon atoms bonded to fluorine in SiO_3F (top), SiO_4F (middle), and SiO_3F_2 (bottom) environments.

coordinated to any Na or Ca, essentially all fluorine is found coordinated to one or more modifier cations.

Figure 4 shows the O and F bond-angle distributions around the modifier atoms. The O−(Na,Ca)−O, O−(Na,Ca)−F and F−(Na,Ca)−F distributions all have the same general shape, with a very broad distribution of angles, indicating a wide range of bonding environments, and peaks at angles of ∼75−90 deg. One would anticipate six-coordinated bonding to be octahedral with bond angles of 90 and 180°; hence, this peak seems to be a distorted version of this expectation. Six is the dominant coordination number for the modifier atoms, with five and seven also contributing strongly, in accordance with the bond-angle distributions. Counting both O and F atoms, we find that the average Na coordination is 6.1, made up of 44% six-coordinated Na, 23% five-coordinated Na and 24% seven-coordinated Na: ^{23}Na MAS NMR experiments also identified multiple (at least two) sodium sites in a fluorinated bioglass composition containing ∼30% CaF_2.[12] Similarly, the average Ca coordination is 6.5, made up of 47% six-coordinated Ca, 35% seven-coordinated Ca, 11% eight-coordinated Ca, and 7% five-coordinated Ca. To the best of our knowledge, despite their high potential for investigating complex biomaterials[53] and silicate glasses,[34] no ^{43}Ca NMR studies have previously involved fluorinated bioglass.

The O−(Na,Ca)−O distributions exhibit a secondary peak at ∼60 degrees, typically associated with modifier ions linking two BOs or two oxygen atoms belonging to two different SiO_4 tetrahedra,[43,54] with smaller angles permitted by the lower repulsion between the two O atoms in these conditions. No such feature is present in the O−(Na,Ca)−F and F−(Na,Ca)−F distributions, as to denote larger repulsion when fluorine is present.

Temperature Dependence of Fluorine Environment. Finally, we investigate the temperature dependence of the fluorine bonding environment, by examining the NVT trajectories of the models as they were being cooled. Figure 5 shows $g_{SiF}(r)$, $g_{NaF}(r)$, and $g_{CaF}(r)$ at temperatures from 300 to 3000 K. For all radial distribution functions we see an evolution from the solid amorphous $g(r)$ at 300 K to a liquid-like $g(r)$ at 2000 K and above, with a characteristic broader first peak, less pronounced first minimum, and less structure at distances greater than that of the first-neighbor shell. There are differences between the modifier cations' behaviors: $g_{NaF}(r)$ barely changes between 2000 K, 2500, and 3000 K, whereas the first peak $g_{CaF}(r)$ continues to get broader as the temperature increases through this range. In one model, we also observed an F−P bond which existed for most of the 2000 K trajectory. It is difficult to examine the coordination number consistently across the temperature range, as the position of the first minimum in the partial $g(r)$'s increases with increasing temperature. Hence, we compute (Table 2) the (Na,Ca)−F coordination numbers both with a cutoff of 3.2 Å (the (Na,Ca)−F cutoff used for the NVE run), and with a cutoff of 3.5 Å, which is the approximate position of the first minimum at the highest temperatures; the similar cutoffs for Si−F are 2.0 and 2.3 Å. Due to the limited statistics in this case, it is difficult to establish firm trends. The error on the Na−F and Ca−F coordination numbers is of the order of 10% of the coordination number itself, which is the same order of magnitude

as the changes in the coordination number with increasing temperature. The Na−F coordination number (cutoff 3.2 Å) decreases by 0.07, and the Ca−F coordination number (cutoff 3.2 Å) decreases by 0.26, implying that there is some evidence for a decrease in the Na−F coordination number, and convincing evidence for a more substantial decrease in the Ca−F coordination number at higher temperatures, which are accompanied by a corresponding increase in the Si−F coordination number.

Examinining the Si−F bonds at high temperature provides further insight into their features: whereas we found no evidence of SiO_4F species[10,21,51] in our final glass structures, the range of silicon coordination numbers and environments increases substantially at higher temperatures, as was also found for F-free bioglass and its melt precursor,[31] and this more varied coordination now includes instances of the five-coordinated SiO_4F complex. In fact, whereas four-coordinated Si atoms dominate at all temperatures (even at 3000 K, 85% of Si atoms are so bonded), the Si−F coordination number increases from 0.07 at 300 K to 0.14 at 3000 K (cutoff 2.3 Å, Table 2), simultaneously with the appearance of three- and five-coordinated Si defects in the melt, above 1000 K (Table 3).

Figure 6 shows the Si−F radial distribution functions for F-bonded Si atoms in three characteristic environments. The most common, SiO_3F (Figure 6 (top)), shows a sharp peak at 1.67 Å, the room-temperature Si−F bond length, which gets wider with increasing temperature. The two other environments, SiO_4F and SiO_3F_2 (Figure 6 (middle) and (bottom)) have a broader range of distances, but the peaks of these distributions are still at roughly the same distance as the room-temperature Si−F bond length. Although the range of the Si−F environments is wide enough to include fluorine atoms bonded at larger distances than (and in addition to) the normal first Si−O coordination shell, it is clear that, at all temperatures studied, the *replacement* of Si−O bonds remains the predominant mechanism of formation of Si−F links. Whereas this is always the most common coordination environment for F-bonded Si, the fraction of F-bonded Si atoms found in the SiO_3F complex decreases with increasing temperature, from 100% at 300 K to 67% at 3000 K, in favor of the two other significantly populated environments, both five-coordinated: SiO_4F and SiO_3F_2. This confirms that the presence of overcoordinated Si in the melt can favor the formation of transient Si−F bonds through the expansion of the SiO_4 coordination shell. Whereas these configurations are less stable and disappear during the cooling of the melt, concurrently with the healing of mis-coordinated Si defects,[31] they can play an important role as intermediates in the process of fluorine migration in the bulk.

CONCLUSIONS

Unbiased *ab initio* molecular dynamics models of the atomic structure of fluorine-containing bioglass allowed us to assess recent suggestions and obtain further insight about key structural features of these materials. Flourine is found predominantly coordinated to the modifier cations, sodium and calcium, with only a small percentage of F−Si bonds, in agreement with some of the previous experiments[12] and simulations.[29] On average, a fluoride ion is found embedded in a mixed shell of modifier Na and Ca cations, whose composition strictly reflects the relative Na/Ca abundance: almost all fluorine atoms are associated with *both* sodium and calcium, and we do not observe any preference for F to coordinate to either Na or Ca. The present simulations, therefore, do not support previous identifications of FM_n clusters, where M is a *single* modifier atom:[8] these aggregates are more likely to be mixed states.

The low stability of Si−F bonds, and the corresponding preferential association of fluoride to modifier ions, will likely lead (on a larger scale) to the formation of alkali-fluoride-rich regions separate from phospho-silicate-rich regions with a more polymerized network compared to the F-free bioglass.[29] Whereas direct observation of this effect is prevented by the small size of the present *ab initio* models, the very different local stability of Si−F vs Na(Ca)-F aggregates highlighted by the present simulations represents a strong indication in favor of this hypothesis. Ion clustering in low-silica regions is associated with enhanced durability and lower bioactivity of glasses,[30,33] hence it is likely to be also one of the reasons behind the reduced or missing formation of the silica gel layer in fluorinated bioglass, and the corresponding observed changes in surface reactivity compared to F-free BG.[13,14] It is interesting to note that the clustering mechanism in FBGs is different from that in F-free bioglasses: in the latter, the higher affinity of calcium for phosphate anions leads to Ca-rich phosphate nanoaggregates separating from Ca-poor silicate regions,[44] whereas in FBGs, fluorine attracts Na and Ca cations in Na,Ca,F-rich domains separated from the phosphosilicate network.

By examining the higher-temperature MD trajectories, we observe decreases in the Na−F and Ca−F coordination numbers, and an increase in the Si−F coordination number with increasing temperature. The dominant environment for Si−F bonds features fluorine replacing one of the oxygen atoms in an SiO_4 tetrahedron at all temperatures. However, as temperature increases, five-coordinated Si atoms with either one or two Si−F bonds occur with increasing frequency. Unlike in other materials, the formation of Si−F bonds through expansion of the tetrahedral Si coordination shell[10,21,51] in fluorine bioglasses seems possible only in conditions which favor coordinative defects, such as high temperature.

AUTHOR INFORMATION

Corresponding Author

*E-mail: a.tilocca@ucl.ac.uk.

Present Addresses

[§]Department of Chemistry, Università di Modena e Reggio Emilia, 41100 Modena, Italy.

ACKNOWLEDGMENT

We are grateful for funding from the U.K.'s Royal Society (University Research Fellowship to A.T.) and EPSRC (Grant No. EP/F020066/1). Through the Materials Chemistry Consortium, this work made use of HPCx and HECToR, the U.K.'s national high-performance computing services; part of the calculations were also performed on the UCL Legion High Performance Computing Facility. A.P. and M.C.M. thank the Italian Ministry of University and Research for funding (project COFIN2008. Prot. 2008J9RNB3 "Integrazione temporale per l'Evoluzione Molecolare").

REFERENCES

(1) Featherstone, J. D. B. *J. Am. Dent. Assoc.* **2000**, *131*, 887.
(2) Hench, L. L. *Science* **1980**, *208*, 826.

(3) Sculean, A.; Barbe, G.; Chiantella, G. C.; Anweiler, N. B.; Berakdar, M.; Brecx, M. *J. Periodont.* **2002**, *73*, 401.
(4) Wood, D.; Hill, R. *Clin. Mater.* **1991**, *7*, 301.
(5) Stebbins, J. F.; Zeng, Q. *J. Non-Cryst. Solids* **2000**, *262*, 1.
(6) Hayashi, M.; Watanabe, T.; Nagata, K.; Hayashi, S. *ISIJ Int.* **2004**, *44*, 1527.
(7) Stamboulis, A.; Hill, R. G.; Law, R. V. *J. Non-Cryst. Solids* **2004**, *333*, 101.
(8) Stamboulis, A.; Hill, R. G.; Law, R. V. *J. Non-Cryst. Solids* **2005**, *351*, 3289.
(9) Kohn, S. C.; Dupree, R.; Mortuza, M. G.; Henderson, C. M. B. *Am. Mineral.* **1991**, *76*, 309.
(10) Hayakawa, S.; Ohtsuki, C.; Matsumoto, S.; Osaka, A.; Miura, Y. *Comput. Mater. Sci.* **1998**, *9*, 337.
(11) Osaka, A.; Wang, Y.-H.; Kobayashi, M.; Miura, Y.; Takahashi, K. *J. Non-Cryst. Solids* **1988**, *105*, 63.
(12) Brauer, D. S.; Karpukhina, N.; Law, R. V.; Hill, R. G. *J. Mater. Chem.* **2009**, *19*, 5629.
(13) Lusvardi, G.; Malavasi, G.; Tarsitano, F.; Menabue, L.; Menziani, M. C.; Pedone, A. *J. Phys. Chem. B* **2009**, *113*, 10331.
(14) Lusvardi, G.; Malavasi, G.; Menabue, L.; Aina, V.; Morterra, C. *Acta Biomater.* **2009**, *5*, 3548.
(15) Clark, T. M.; Grandinetti, P. J.; Florian, P.; Stebbins, J. F. *Phys. Rev. B* **2004**, *70*, 064202.
(16) Angelopoulou, A.; Montouillout, V.; Massiot, D.; Kordas, G. *J. Non-Cryst. Solids* **2008**, *354*, 333.
(17) Coelho, C.; Azais, T.; Bonhomme-Coury, L.; Laurent, G.; Bonhomme, C. *Inorg. Chem.* **2007**, *46*, 1379.
(18) Gunawidjaja, P. N.; Lo, A. Y. H.; Izquierdo-Barba, I.; García, A.; Arcos, D.; Stevensson, B.; Grins, J.; Vallet-Regí, M.; Edén, M. *J. Phys. Chem. C* **2010**, *114*, 19345.
(19) Martineau, C.; Body, M.; Legein, C.; Silly, G.; Buzaré, J.-Y.; Fayon, F. *Inorg. Chem.* **2006**, *45*, 10215.
(20) Pulido, A.; Corma, A.; Sastre, G. *J. Phys. Chem. B* **2006**, *110*, 23951.
(21) Fyfe, C. A.; Brouwer, D. H.; Lewis, A. R.; Villaescusa, L. A.; Morris, R. E. *J. Phys. Chem. B* **2006**, *110*, 23951.
(22) Attfield, M. P.; Catlow, C. R. A.; Sokol, A. A. *Chem. Mater.* **2001**, *13*, 4708.
(23) Camblor, M. A.; Diaz-Cabanas, M. J.; Perez-Pariente, J.; Teat, S. J.; Clegg, W.; Shannon, I. J.; Lightfoot, P.; Wright, P. A.; Morris, R. E. *Angew. Chem., Int. Ed.* **1998**, *37*, 2122.
(24) Sastre, G.; Gale, J. D. *Chem. Mater.* **2005**, *17*, 730.
(25) Hench, L. L.; Ethridge, E. C. *Biomaterials: an interfacial approach*; Academic Press: San Diego, CA, 1982.
(26) Hench, L. L. *J. Biomed. Mater. Res.* **1998**, *41*, 511.
(27) Zaffe, D.; Krajewski, A.; Ravaglioli, A.; Contoli, S. *J. Mater. Sci.: Mater. Med.* **1993**, *4*, 169.
(28) Ebisawa, Y.; Kokubo, T.; Ohura, K.; Yamamuro, T. *J. Mater. Sci.: Mater. Med.* **1990**, *1*, 239.
(29) Lusvardi, G.; Malavasi, G.; Cortada, M.; Menabue, L.; Menziani, M. C.; Pedone, A.; Segre, U. *J. Phys. Chem. B* **2008**, *112*, 12730.
(30) Christie, J. K.; Tilocca, A. *Chem. Mater.* **2010**, *22*, 3725.
(31) Tilocca, A. *Phys. Rev. B* **2007**, *76*, 224202.
(32) Christie, J. K.; Tilocca, A. *Adv. Engin. Mater.* **2010**, *12*, B326.
(33) Tilocca, A. *J. Mater. Chem.* **2010**, *20*, 6848.
(34) Pedone, A.; Charpentier, T.; Menziani, M. C. *Phys. Chem. Chem. Phys.* **2010**, *12*, 6054.
(35) Tilocca, A.; Cormack, A. N. *Langmuir* **2010**, *26*, 545.
(36) Tilocca, A. *J. Chem. Phys.* **2008**, *129*, 084504.
(37) Giannozzi, P.; et al. *J. Phys.: Condens. Mat.* **2009**, *21*, 395502.
(38) Perdew, J. P.; Burke, K.; Ernzerhof, M. *Phys. Rev. Lett.* **1996**, *77*, 3865.
(39) Vanderbilt, D. *Phys. Rev. B* **1990**, *41*, 7892.
(40) Tilocca, A.; de Leeuw, N. H.; Cormack, A. N. *Phys. Rev. B* **2006**, *73*, 104209.
(41) Tilocca, A.; de Leeuw, N. H. *J. Mater. Chem.* **2006**, *16*, 1950.
(42) Tilocca, A.; Cormack, A. N. *J. Phys. Chem. C* **2008**, *112*, 11936.
(43) Tilocca, A.; de Leeuw, N. H. *J. Phys. Chem. B* **2006**, *110*, 25810.
(44) Tilocca, A.; Cormack, A. N. *J. Phys. Chem. B* **2007**, *111*, 14256.
(45) Pedone, A. *J. Phys. Chem. C* **2009**, *113*, 20773.
(46) Pota, M.; Pedone, A.; Malavasi, G.; Durante, C.; Cocchi, M.; Menziani, M. C. *Comput. Mater. Sci.* **2010**, *47*, 739.
(47) Sarnthein, J.; Pasquarello, A.; Car, R. *Phys. Rev. Lett.* **1995**, *74*, 4682.
(48) Giacomazzi, L.; Massobrio, C.; Pasquarello, A. *Phys. Rev. B* **2007**, *75*, 174207.
(49) Du, J.; Corrales, L. R. *J. Chem. Phys.* **2006**, *125*, 114702.
(50) FitzGerald, V.; Pickup, D. M.; Greenspan, D.; Sarkar, G.; Fitzgerald, J. J.; Wetherall, K. M.; Moss, R. M.; Jones, J. R.; Newport, R. J. *Adv. Func. Mater.* **2007**, *17*, 3746.
(51) Corma, A.; Puche, M.; Rey, F.; Sankar, G.; Teat, S. J. *Angew. Chem., Int. Ed.* **2003**, *42*, 1156.
(52) Coelho, C.; Azais, T.; Bonhomme-Coury, L.; Maquet, J.; Massiot, D.; Bonhomme, C. *J. Magn. Reson.* **2006**, *179*, 114.
(53) Laurencin, D.; Gervais, C.; Wong, A.; Coelho, C.; Mauri, F.; Massiot, D.; Smit, M. E.; Bonhomme, C. *J. Am. Chem. Soc.* **2009**, *131*, 13430.
(54) Tilocca, A. *J. Chem. Phys.* **2010**, *133*, 014701.